Biomass burning contributions estimated by synergistic coupling of daily and hourly aerosol composition records

S. Nava [a,*], F. Lucarelli [a], F. Amato [c], S. Becagli [b], G. Calzolai [a], M. Chiari [a], M. Giannoni [b], R. Traversi [b], R. Udisti [b]

[a] I.N.F.N.-Florence and Department of Physics and Astronomy, University of Florence, Via Sansone 1, 50019, Sesto Fiorentino (FI), Italy
[b] Department of Chemistry, University of Florence, Via della Lastruccia 3, 50019, Sesto Fiorentino (FI), Italy
[c] Institute of Environmental Assessment and Water Research (IDÆA), Spanish National Research Council (CSIC), C/Jordi Girona 18-26, 08034 Barcelona, Spain

HIGHLIGHTS

• PMF has been applied to both daily and hourly aerosol compositional data-sets.
• Unexpectedly very high biomass burning contributions were found in Central Italy.
• Multi-elemental high time resolved PIXE data allowed a clear source identification.

ARTICLE INFO

ABSTRACT

Biomass burning (BB) is a significant source of particulate matter (PM) in many parts of the world. Whereas numerous studies demonstrate the relevance of BB emissions in central and northern Europe, the quantification of this source has been assessed only in few cities in southern European countries. In this work, the application of Positive Matrix Factorisation (PMF) allowed a clear identification and quantification of an unexpected very high biomass burning contribution in Tuscany (central Italy), in the most polluted site of the PATOS project. In this urban background site, BB accounted for 37% of the mass of PM10 (particulate matter with aerodynamic diameter <10 μm) as annual average, and more than 50% during winter, being the main cause of all the PM10 limit exceedances.

Due to the chemical complexity of BB emissions, an accurate assessment of this source contribution is not always easily achievable using just a single tracer. The present work takes advantage of the combination of a long-term daily data-set, characterized by an extended chemical speciation, with a short-term high time resolution (1-hour) and size-segregated data-set, obtained by PIXE analyses of streaker samples. The hourly time pattern of the BB source, characterised by a periodic behaviour with peaks starting at about 6 p.m. and lasting all the evening-night, and its strong seasonality, with higher values in the winter period, clearly confirmed the hypothesis of a domestic heating source (also excluding important contributions from wildfires and agricultural wastes burning).

© 2014 Elsevier B.V. All rights reserved.

1. Introduction

Biomass burning (BB), which is generally defined as combustion of any non-fossilized vegetative or organic fuel, is a significant source of particulate matter (PM) in many parts of the world: on a global scale, it is the largest source of primary fine carbonaceous aerosols (Akagi et al., 2011). The use of BB for domestic heating is increasing in many European countries, as it is considered a renewable energy source and it is in general less expensive than methane and oil combustion. The

recent economical crisis further pushed the domestic use of wood (and similar materials) burning.

In the last years, many studies have been carried out to evaluate the BB contribution to PM because of its impact on air quality, human health, and climate change (Szidat et al., 2007, 2009; Gelencsér et al., 2007; Piazzalunga et al., 2011, Saarikoski et al., 2008; Viana et al., 2013). However, when several sources are simultaneously responsible of air pollution, it is often difficult to unravel the different contributions and to assess the impact of BB source only. The use of different kinds of biomass fuels (wood chips, bark, waste wood, straw, etc.) and different combustion technologies (operating at different temperatures) is reflected by the large variability of source profiles reported in literature for this source. Moreover, the reactivity, the volatility and to some extent the hygroscopicity of organic compounds, including also main BB

tracers like levoglucosan, may compromise the basic assumptions for receptor models and strongly increase difficulties and uncertainties in source apportionment.

Next to carbonaceous particles, which dominated biomass burning emissions especially in the older and less efficient combustion systems, many inorganic elements-compounds are emitted by these processes, like potassium salts (KCl, K_2SO_4, KNO_3, K_2CO_3), metals (Zn, Pb) and also refractory compounds including the elements Ca, Mg and Si (Jöller et al., 2007; Khalil and Rasmussen, 2003; Christensen et al., 1998; Obernberger, 1998). Although there are several potential chemical markers, an easy assessment of this source contribution using a single specific (and robust) tracer is hampered by the chemical complexity of these emissions. In this context, multi-elemental composition measurements can be very useful. In particular, the possibility of measuring elemental concentrations with high time resolution may be of great help in disentangling the contribution of this source by means of receptor models, like Positive Matrix Factorisation (PMF).

In the framework of the regional project PATOS (Particolato Atmosferico in TOScana), PM has been collected in 6 sampling sites in Tuscany both with daily and hourly time resolution: daily PM10 (i.e. particulate matter with aerodynamic diameter <10 μm) samples have been collected for 1 year and analysed by different techniques in order to obtain a complete chemical composition characterization (elements, ions, elemental and organic carbon); hourly fine (<2.5 μm) and coarse (2.5-10 μm) PM samples have been collected for shorter periods by the Streaker sampler and hourly elemental concentrations have been obtained by Particle Induced X-ray Emission (PIXE) analysis. Unexpectedly, the urban background site of Capannori, a small town near Lucca, resulted to be the most polluted among the sampling sites, with average PM10 concentration and number of daily exceedances even higher then those registered in the kerb sites.

In this paper, results concerning the BB source identification and characterisation in this highly polluted sampling site will be shown, with some comparison with the other sites of the PATOS project. To our best knowledge, whereas a discrete number of studies on BB have been accomplished in Northern Italy (Bernardoni et al., 2011, 2013; Pastorello et al., 2011; Piazzalunga et al., 2011), this is the first time that a strong impact of BB is demonstrated for central Italy. More in general, while numerous studies demonstrate the relevance of BB emissions on PM in many urban and suburban environments in central and northern Europe (see for example, Puxbaum et al., 2007; Saarikoski et al., 2008; Szidat et al., 2009; Favez et al., 2009), the quantification of this source has been assessed only in few cities in southern Europe (Alves et al., 2011; Gonçalves et al., 2012; Karanasiou et al., 2009; Minguillón et al., 2011; Reche et al., 2012; Viana et al., 2013). Only in one recent study (Giannoni et al., 2012), levoglucosan has been used to trace biomass burning in PM2.5 samples collected in Tuscany (Florence and Livorno): relatively high levoglucosan concentrations, similar to those reported for northern Italy, were found in the cold season, thus suggesting a possible significant impact of domestic heating; however contributions to PM were not quantified.

2. Methods

Aerosol samples were collected from September 2005 to September 2006, in six sampling sites in Tuscany (Central Italy) representative of areas with different characteristics (Fig. S1): Florence – urban background (FL_UB), Prato – traffic site (PO_TS), Capannori (Lucca) – urban background (CA_UB), Arezzo – traffic site (AR_TS), Grosseto – urban background (GR_UB) and Livorno – suburban/rural background (LI_SB). About 1000 PM10 samples were collected on a daily basis (from midnight to midnight) by three low volume (2.3 m³/h) samplers (HYDRA Dual Sampler), each of them equipped with two inlets in order to simultaneously collect the aerosol on Teflon and Quartz fibre filters.

The samplers were relocated every 15 days from three sampling sites (FL_UB, CA_UB and GR_UB) to the other three (AR_TS, PO_TS and LI_SB).

PM10 daily mass concentrations were obtained by weighing the Teflon filters by an analytical balance in controlled conditions of temperature (20 ± 1 °C) and relative humidity (50 ± 5 %). Samples collected on Teflon filters were then analysed by PIXE (Lucarelli et al., 2010, 2014) to measure the concentrations of all the elements with atomic number $Z > 10$ with the external set-up described in Calzolai et al. (2006), by Ion Cromatography (IC) to quantify the soluble component (sample extraction in ultra-pure MilliQ water in ultrasonic bath) of inorganic cations, inorganic anions and low molecular weight organic anions (Becagli et al., 2011), and by Inductively Coupled Plasma Atomic Emission Spectroscopy (ICP-AES) to assess the soluble component (sample extraction in ultrasonic bath with MilliQ water acidified at pH 1.5–2 with ultra-pure nitric acid) of selected metals (Traversi et al., 2014). Samples collected on Quartz fibre filters were analysed by a CHN Analyzer (Thermo 1112) to measure Total Carbon (TC) concentration and estimate Elemental Carbon (EC) and Organic Carbon (OC) components according to the method proposed by Zappoli et al. (1999).

In particular, ~400 daily samples (~200 on Teflon and ~200 on Quartz fibre filters) were collected and analysed for the CA_UB site.

During shorter periods (1-2 weeks for each site) the aerosol was also collected by a low volume (0.06 m³/h) two-stage streaker sampler (D'Alessandro et al., 2003; Crespo et al., 2010; Amato et al., 2011; Dall'Osto et al., 2013). Briefly, in this device, particles are separated on different stages by a pre-impactor and an impactor. The pre-impactor removes PM with aerodynamic diameter $D_{ae} > 10$ μm. The impactor deposits the aerosol coarse fraction (2.5 μm < D_{ae} < 10 μm) on a Kapton foil while the fine fraction (D_{ae} < 2.5 μm) is collected on a Nuclepore filter. The two collecting substrata (Kapton and Nuclepore) are paired on a cartridge which rotates at constant speed for a week: this produces a circular continuous deposition of particulate matter ("streak") on both stages. PIXE analysis of these samples by a properly collimated proton beam, scanning the deposit in steps corresponding to 1 h of aerosol sampling, provided the elemental concentrations with hourly time resolution (Lucarelli et al., 2010).

Positive Matrix Factorisation (PMF) has been applied to the whole data set (separately on daily and hourly samples) aiming at the identification and the quantification of the major aerosol sources, using the EPA PMFv3 software. PMF is an advanced factor analysis technique based on a weighted least square fit approach (Paatero and Tapper, 1994); it uses realistic error estimates to weigh data values and imposes non-negativity constraints in the factor computational process. Briefly, the PMF factor model may be written as $X = G \cdot F + E$, where X is a known n by m matrix of the m measured chemical species in n samples; G is an n by p matrix of source contributions to the samples (i.e. time variations of the p factor scores); F is a p by m matrix of factors composition (often called source profiles). E is defined as a residual matrix: it represents the difference between the measured concentrations (X) and those reproduced by the model (G · F). The PMF objective is determining the G and F factor matrices that minimize the sum of the squares of the inversely weighed residuals with uncertainty estimates of the data points. Furthermore, PMF constrains all the elements of G and F to be non-negative, meaning that sources cannot have negative species concentration ($f_{kj} \geq 0$) and samples cannot receive a negative source contribution ($g_{ik} \geq 0$).

Input data were prepared using the procedure suggested by Polissar (Polissar et al., 1998) and PMF results for different number of factors and multiple values of FPEAK were systematically explored to find out the most reasonable solution (20 pseudorandom initializations were run for each test).

For daily samples, G and F matrices were normalized by multilinear regression analysis, i.e. by regressing the total PM10 mass concentration measured for each sample against the factor scores, to obtain absolute source profiles and contributions. For hourly data, only elemental

concentrations were measured and no information about the PM mass concentration is available: in this case, only relative source profiles (elemental ratios within the composition of the identified sources) can be obtained and source time series are expressed in arbitrary units.

3. Results and discussion

3.1. Daily data: PM10 concentration and composition

In Fig. 1 the annual and seasonal box and whisker plots of PM10 concentration, for all the sampling sites, are shown. As it can be seen, the higher PM10 concentrations are measured in CA_UB (annual average value: 41.1 µg/m³): despite its classification as an urban background station, CA_UB is characterised by PM10 levels even higher than those measured in the two traffic sites (AR_TS and PO_TS). When seasonal values are explored, PM10 concentration in CA_UB appears to be significantly higher than those of the other sampling sites during in winter; a lower difference can be observed in spring and autumn, while the summer average is very similar to those found in the other sites.

Average concentrations of main measured elements/species for all the sampling sites are reported in supplementary material (Table S1). In comparison with all the other sites, CA_UB is characterised by higher concentrations mainly of OC, K and K^+, acetates, glycolates, formates, Ca and Ca^{2+}, Zn and Pb (but also EC and Cu, if traffic sites are excluded, and Cl and Br, if the costal site of LI_SB is not taken into account). Monthly averages of OC and K in CA_UB are shown in Fig. 2, together with the minimum-maximum range of the concentration of these species in the other sampling sites. Significantly higher values in CA_UB are evident from November to March, while concentrations observed during the rest of the year are similar to those found in the other sampling sites. The same behaviour holds true for the other aforementioned species (K^+, acetates, glycolates, formates, Ca, Ca^{2+}, Zn, Pb) as shown in the supplementary material (Fig. S2).

To better understand the origin of these high K concentrations in Capannori, Enrichment Factors (EFs) were calculated with respect to Al, using the mean crust composition profile reported in Mason (1966), and total K concentration obtained by PIXE was compared to the K^+ ion soluble fraction as measured by IC. Whereas K from biomass burning is entirely soluble in water (it is mostly present as KCl and K_2SO_4), K from mineral dust is not soluble (Maenhaut et al., 2011). Results are shown, as monthly averages, in Fig. 3, where a clear seasonal trend may be observed: during winter ~80% of K is soluble and quite high EFs are observed, while a lower solubility and a lower enrichment
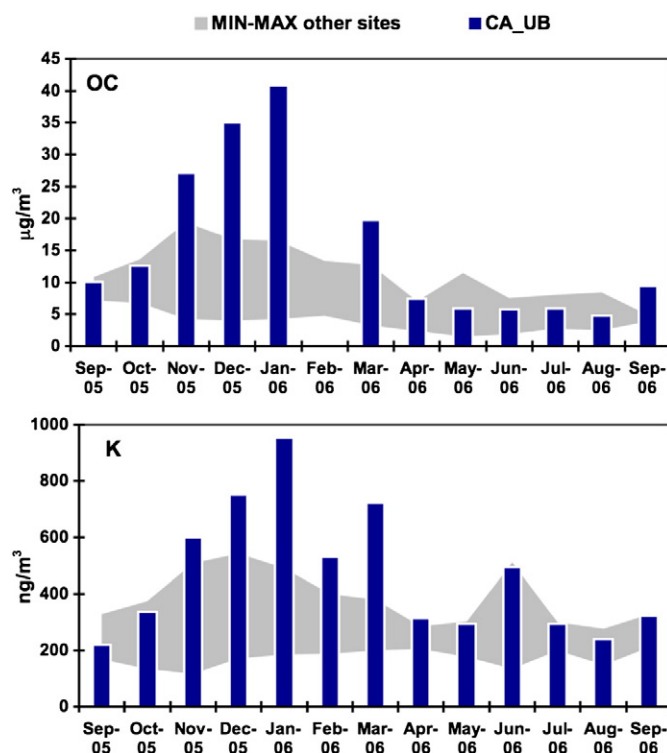

Fig. 2. Monthly averages of OC and K in the CA_UB site (OC concentration in February not available due to malfunctioning of the Quartz filter sampling line); the minimum-maximum range of concentration in the other sampling sites is also show for comparison.

are observed in summer (the very low value in June for both EF and solubility has to be ascribed to a strong Saharan dust episode, which lasted several days (Nava et al., 2012; Calastrini et al., 2012)). A high correlation between K and K^+ ($r^2 = 0.94$) is indeed observed during winter (Fig. 4). All these results point out at a significant non-soil contribution to K during the cold season, suggesting the possible impact of biomass burning.

This hypothesis is clearly reinforced by the fact that other chemical species (OC, acetates, glycolates, formates, Ca and Ca^{2+}, Zn, Pb, EC, Cu, Cl and Br) which are characterised by high wintertime concentration values in CA_UB (with respect to the other sampling sites) may be also produced by biomass burning, as previously reported (Jöller et al.,
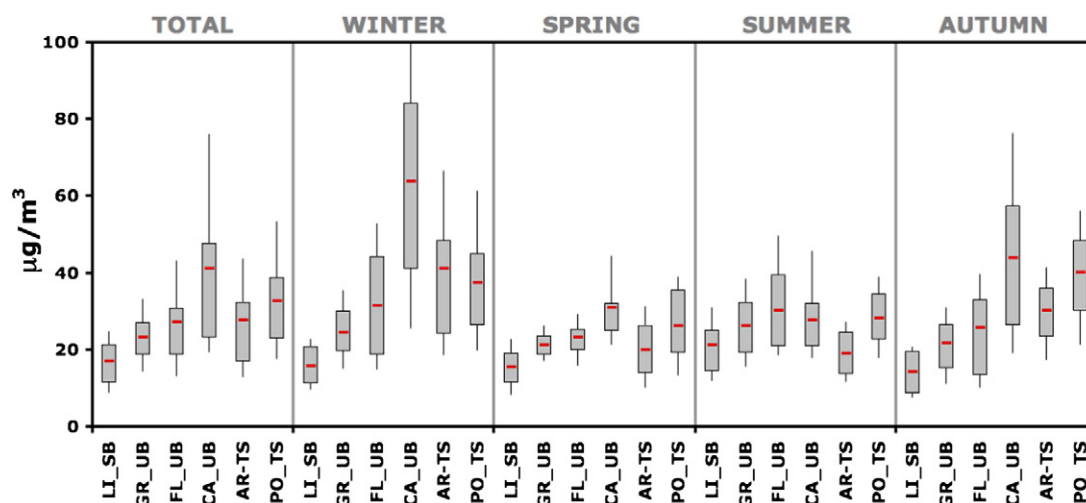

Fig. 1. Box and whisker plot of the PM10 concentration in the 6 sampling sites: Florence – urban background (FL_UB), Prato – traffic site (PO_TS), Capannori (Lucca) – urban background (CA_UB), Arezzo – traffic site (AR_TS), Grosseto – urban background (GR_UB) and Livorno – suburban/rural background (LI_SB). Boxes indicate the inter-quartile range, red dots are average values and the ends of the whiskers represent the 10th and 90th percentiles.
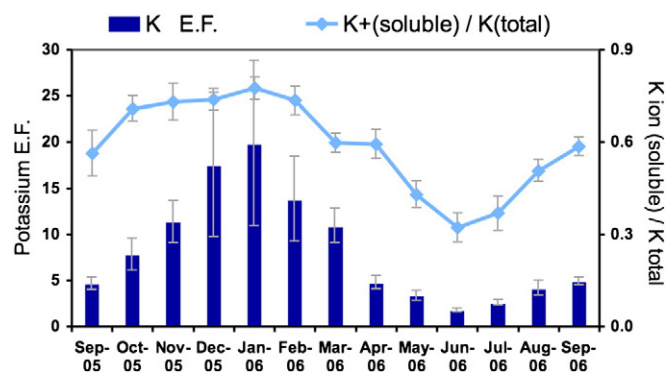
Fig. 3. Monthly averages of K enrichment factors (E.F.) and concentration ratio between soluble K⁺ ion (measured by IC) and total K (measured by PIXE); grey bars represent sample variability (1 standard deviation).

2007; Khalil and Rasmussen, 2003; Christensen et al., 1998; Obernberger, 1998). These species resulted indeed highly correlated to K⁺ (for example, OC: $r^2 = 0.86$ and Glycolate: $r^2 = 0.75$, Fig. 4). The presence of a biomass burning source is also compatible with the observed quite high OC/EC ratios, ranging from 0.3 to 17 with an average value of 6.7 (Fig. 4). It is indeed known that BB usually produces higher OC/EC ratios (5-15) than gasoline or diesel vehicles (Bernardoni et al., 2011; Piazzalunga et al., 2011; Szidat et al., 2006).

3.2. Elemental hourly data

The use of the Streaker sampler allowed obtaining high time resolved and size segregated data, i.e. the elemental concentrations with hourly time resolution in the fine and coarse aerosol fractions, for one week during the winter season (from January 20 to January 27). As shown in Fig. 5, K time series in the fine and coarse fractions are very different. In the fine fraction, the temporal trend of K is characterised by a periodic pattern with peaks starting at about 18:00 and lasting several hours. The same time structure may be observed in the time series of other elements in the fine fraction, especially Cl (correlation coefficient $r = 0.95$) and, to a lesser extent, Br ($r = 0.74$), Pb ($r = 0.68$), S ($r = 0.66$), Cu ($r = 0.64$) and Zn ($r = 0.80$). A different

behaviour can be observed for the coarse fraction: in this fraction K is mainly correlated with other crustal elements (Mg: $r = 0.77$, Al: $r = 0.82$, Si: $r = 0.81$, Ca: $r = 0.77$, Ti: $r = 0.81$, Mn: $r = 0.88$, Fe: $r = 0.73$), while Cl is, for example, correlated with the other sea salt elements (such as Na, see Fig. 5).

It is worth noticing that during this January sampling week, the K concentration is markedly higher in the fine fraction (average: 1.30 μg/m³, with peak values up to 5-6 μg/m³) than in the coarse one (average: 0.06 μg/m³, with peak values up to 0.25 μg/m³). These data confirm the presence of a significant non-soil (and non-sea spray as well) contribution to potassium in winter. Moreover, the time pattern of K in the fine fraction, showing periodic peaks in the late evening-night, clearly suggests the presence of a domestic heating biomass burning source, and also the correlation with Cl, Br, Pb, S, Cu and Zn is consistent with this hypothesis. The absence of the evening-night peak on January 23 may be probably explained by meteorological conditions, as it was the only windy night of the week (Fig. S3). From 6:00 on January 23 to 17:00 on January 24 a quite strong wind (2-5 m/s) blew from east (Fig. S3), and the concentrations of typical sea-spray elements increased (see Na and Cl time trends in Fig. 5), thus suggesting the incoming of external air masses from the Adriatic Sea (back trajectory calculations confirmed this hypothesis). It is also interesting to note that the days with the highest fine K concentrations are the weekend ones (January 21-22, 2006), i.e. when people spend more time at home. In particular, Saturday was characterized by the highest evening peak and also by significant concentration values during the day; it was indeed a very cloudy and cold Saturday (see Fig. S3 in supplementary material), with a slight of precipitation (0.2 mm) during a couple of hours (12:00-13:00).

A completely different time pattern can be observed for other elements. For example, the time series of Fe and Cu, which are markers of traffic emissions (Amato et al., 2011; Dall'Osto et al., 2013), are highly correlated and they feature by a periodic behaviour with peaks during traffic rush hours in the working days and by the absence of the morning peak on Sunday (Fig. 5, third panel).

3.3. PMF results

As previously mentioned, PMF analysis was carried out separately on the daily and the hourly data sets of CA_UB. In the case of the daily PM10
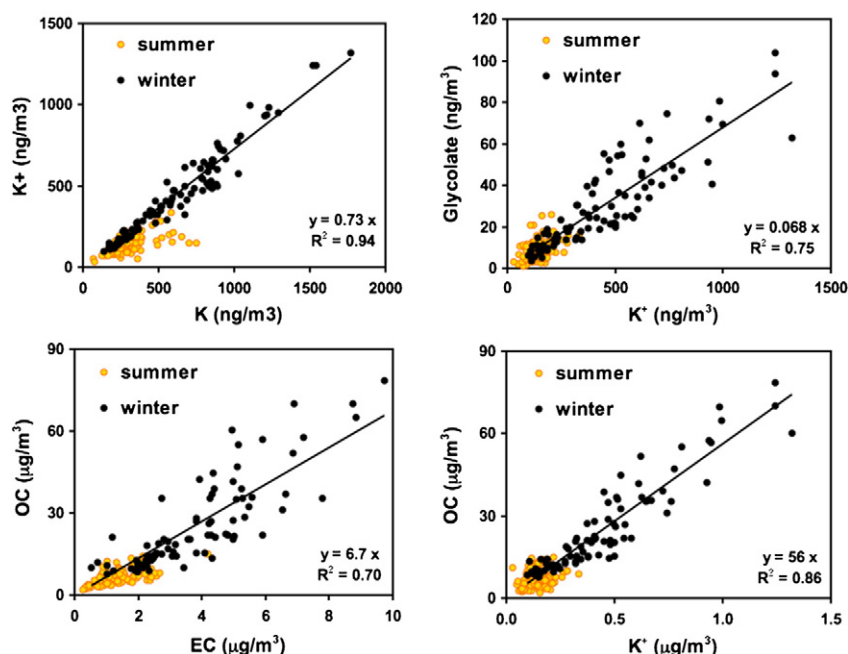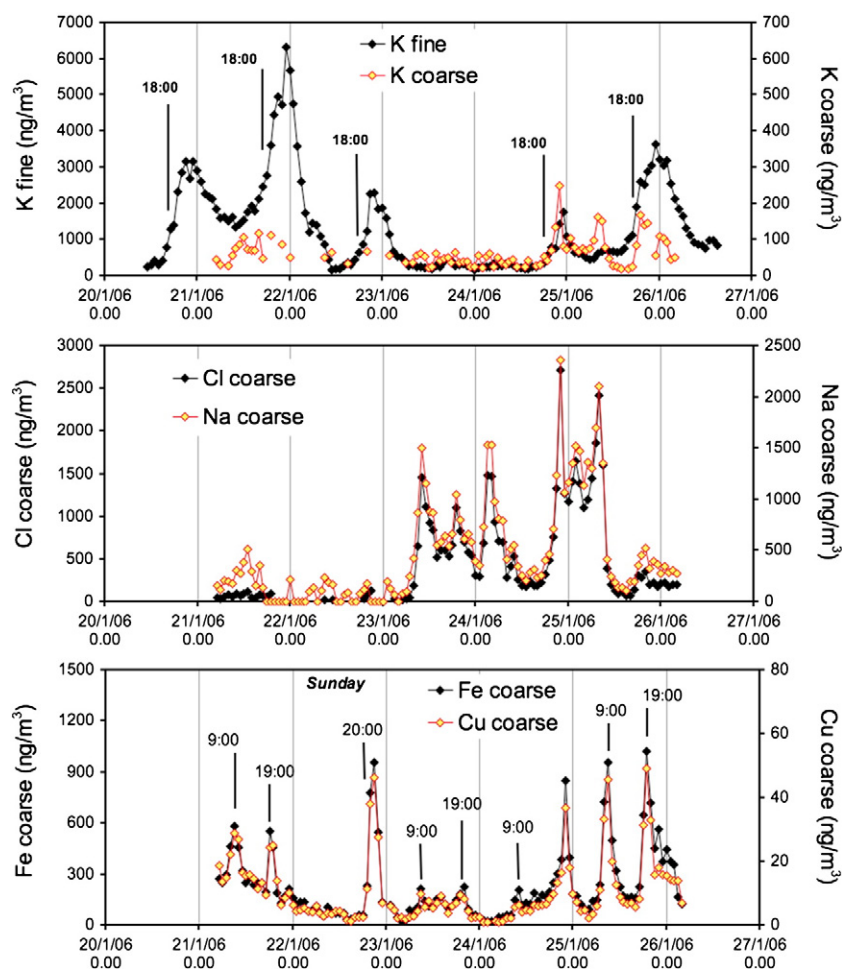

Fig. 4. Concentration scatterplots for some pairs of species, for winter and summer samples collected in the CA_UB site. The regression line and the equation for winter data are also shown.

Fig. 5. Hourly concentration time series of K in the fine and coarse fractions (upper panel), Na and Cl in the coarse fraction (central panel), and Fe and Cu in the coarse fraction (lower panel) in the CA_UB site.

dataset (25 variables, 182 cases), a 7-factor solution with FPEAK = 0 has been selected. Most of the scaled residuals are between ± 3.0, with a random distribution of positive and negative values, and concentrations of all species are reconstructed within ± 11% by the model. Absolute source profiles and contributions have been obtained by regressing the PM10 mass concentration measured for each sample against the factor scores: the adjusted R^2 is 0.96 and all regression coefficients are positive, with p-values below 10^{-5}. The scatterplot between reconstructed and measured PM10 concentrations is shown in Fig. S4. Increasing the number of factors produced inconsistent mass balances, i.e. the sum of the contributions of input species largely exceeded 100% of the total mass in some factor profiles (while other profiles were unreasonably poorly reconstructed).

On the basis of their chemical profiles and time series, PMF factors have been assigned to aerosol sources. Among the identified sources, one is clearly associated to biomass burning, while the others are: traffic, soil dust, secondary sulphates, secondary nitrates, fresh and aged sea salt. Source profiles are shown in Fig. 6: the contribution of each species to the chemical profile composition of each source is reported (ng/ng, grey bars) as well as the average percentage contribution of each source to the concentration of each element (%, black points). Fig. 7 shows the time series plots of daily source contributions to PM10 mass concentration, from each source. Average source contributions to PM10 are reported in Fig. 8 (as absolute concentrations, expressed in μg/m³) and in Table S2 (as % of PM10 concentration), for the whole sampling period and for the different seasons; source contributions were also averaged over all the days when the 50 μg/m³ PM10 limit was exceeded.

The biomass burning profile is characterised by EC, OC, K, Cl, acetate, glycolate, formate and, to a lesser extent, by Cu, Zn, Br, Pb and nitrate (Fig. 6). OC and EC provide the main contribution to the source mass concentration, namely 61% and 8%, respectively. On the other hand, this source explains 42% of EC, 57% of OC, 37% of K, 22% of Cl, 64% of acetate, 69% of glycolate, 47% of formate, 21% of Cu, 18% of Zn, 16% of Br, 18% of Pb and 18% of nitrates. The OC/EC ratio in this profile (8.1) is within the ranges reported in literature for BB (see for example, Bernardoni et al., 2011; Piazzalunga et al., 2011; Szidat et al., 2006). As discussed in Section 3.1, these elements/compounds are those showing a higher winter concentration in CA_UB with respect to the other sampling sites in Tuscany, and, as previously mentioned, they may be considered as markers of biomass burning. Potassium and chlorine are major ions emitted from straw and other agricultural residue burning (Christensen et al., 1998; Sillapapiromsuk et al., 2013). In the combustion of chemically untreated wood chips, compounds of K, S and Cl dominate the inorganic aerosol fraction, but during bark and waste wood combustion also Zn and Pb may become relevant (Jöller et al., 2007). Also Br may be produced by BB and it has been indeed considered as a marker of this source together with K in previous studies (Andreae et al., 1996; Corrigan et al., 2013). In general, it is known that plants take up metals from the soils and can enrich some of them to high levels (Reimann et al., 2008). Carboxylic acids represent an important group of organic compounds identified in the atmospheric aerosol (Rogge et al., 1993). In particular, formic and acetic acids are the dominant species of the organic acids in the tropospheric aqueous and gaseous phases, and are also present in aerosol particles (Grosjean, 1992). Many anthropogenic and natural inputs are acknowledged for
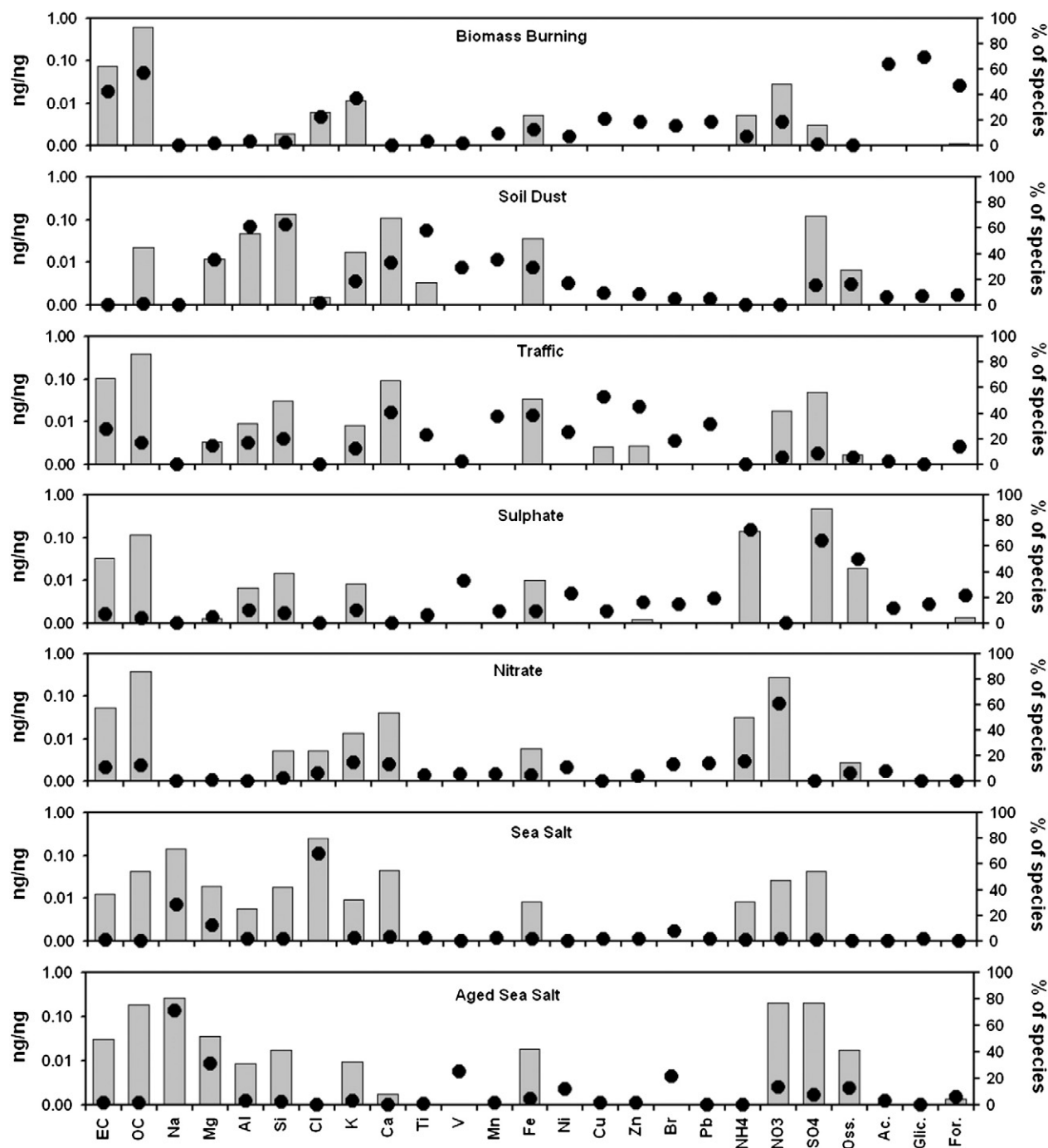
Fig. 6. Source profiles obtained by PMF analysis of daily PM10 samples collected in the CA_UB site.

these compounds and, among them, the most relevant ones are the traffic emissions, soil and vegetation inputs, coal/waste/biomass burning and secondary atmospheric formation from gas-phase precursors (Wang et al., 2007).

The temporal trend of this source features a very strong seasonal pattern with higher values during the cold season (Fig. 7), supporting its interpretation as a BB source for domestic heating.

The traffic source is typified by EC, Cu, Zn, Fe, Mn, Ca, Pb and, to a lesser extent, by OC, Al, Si and Ti (Fig. 6). On the basis of its profile, this factor has been interpreted as a traffic contribution which includes both exhaust and non-exhaust emissions. EC is indeed due to primary exhaust emission, Cu and Fe are well known makers of brake wear, Zn is used as an additive in lubricating oil, while Ca and other mineral elements are produced by road dust resuspension (Amato et al., 2010,

Viana et al., 2008). A moderate seasonal pattern is observed in the estimated contributions of this source to PM10 concentrations, showing lower concentrations in summer (Fig. 8, Table S2).

The soil dust source profile is mainly characterised by Al, Si and Ti, well-known markers of mineral dust, and, to a lesser extent, by other typical crustal elements, like Mg, K, Ca, Mn and Fe (Fig. 6). Enrichment factors (EF) in this profile, calculated with respect to Al using the average continental crust composition (Mason, 1966), are all near 1 and namely: 0.95 (Mg), 0.83 (Si), 1.15 (K), 5.0 (Ca), 1.3 (Ti), 1.5 (Mn) and 1.2 (Fe), thus strengthening the identification of this source as "mineral dust" (if the crust-air fractionation is taken into account (Rahn, 1976) and a reference Si/Al ratio of 2.79 is used instead of the 3.4 ratio reported in (Mason, 1966), the Si EF becomes exactly 1.0). The relatively higher EF of Ca may be due to the specific composition
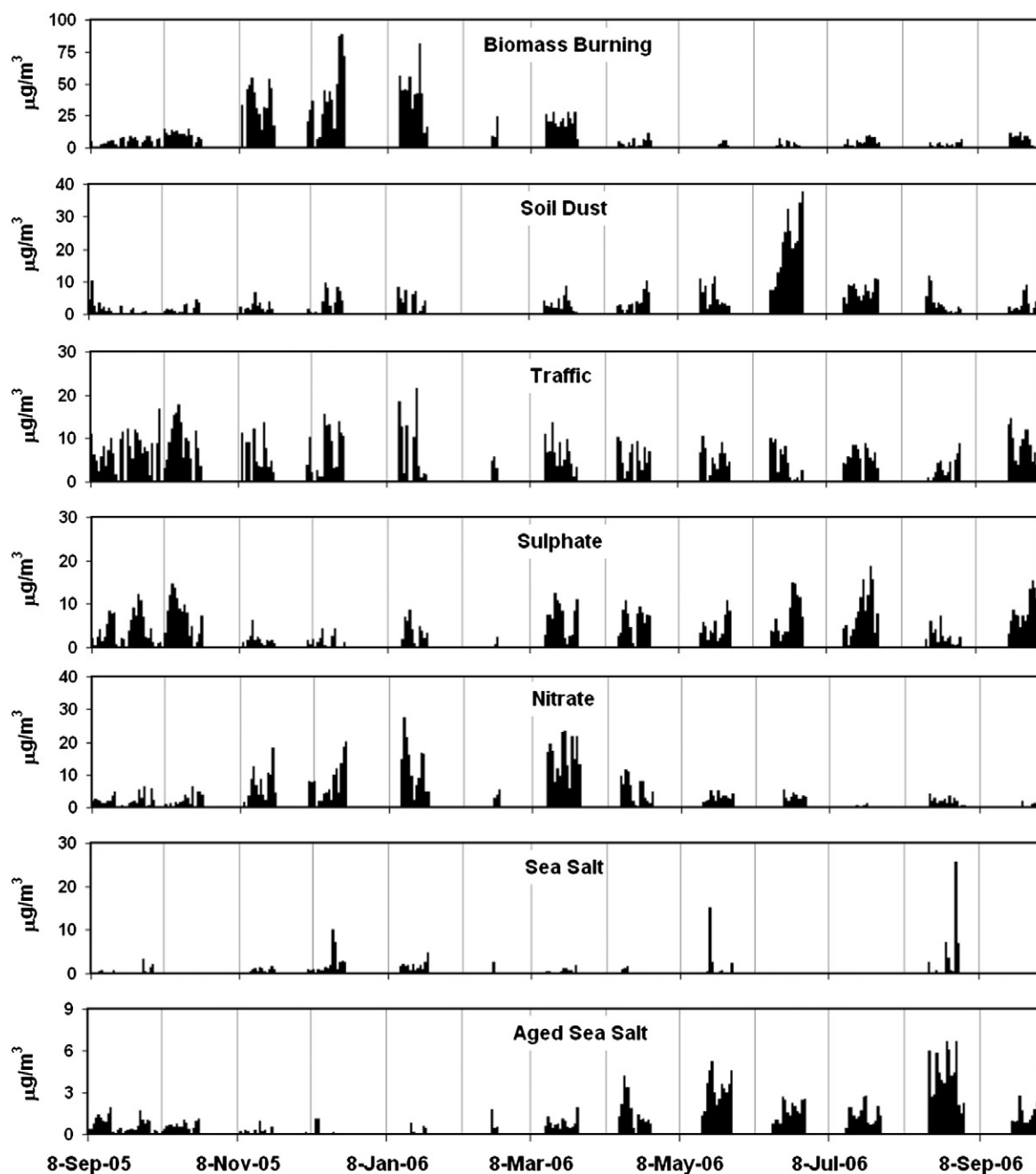
Fig. 7. Time series of source contributions obtained by PMF analysis of daily PM10 samples collected in the CA_UB site.
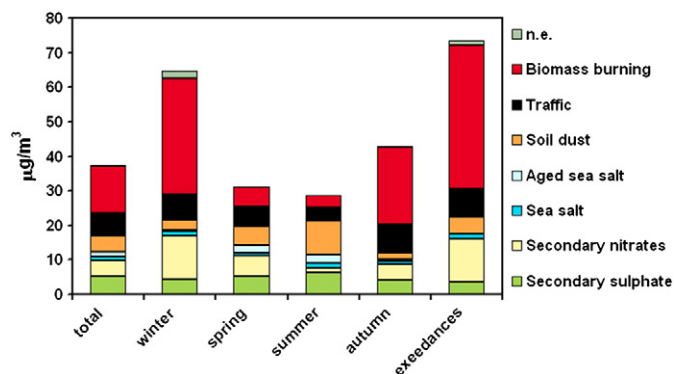

Fig. 8. Average source contributions to PM10 during the whole sampling period, in the different seasons, and during days when the 50 μg/m³ limit was exceeded.

of the local mineral dust, but also to contaminations from construction works and/or asphalt abrasion. This source also includes the contribution of long range transported mineral dust from the Sahara desert. In particular, the high concentration values during June 19-28, 2006 (~20-30 μg/m³) have to be ascribed to a strong and long-lasting Saharan intrusion (Nava et al., 2012); the only PM10 exceedances that occurred during summer were due to this event.

The secondary sulphates source is traced by sulphates and ammonium, which together account for about 62% of the mass in the factor profile, and, to a lesser extent, by oxalates, V and Ni (Fig. 6). OC is also a significant contributor (~10%), but much less than in other factors. Oxalates contain carbon at highest oxidation level among the carboxylic acids and are related to the oxidative capacity of atmosphere: for this reason they are present in the same factor of sulphate. V and Ni are commonly associated to heavy-oil combustion for power generation (Pacyna and Pacyna, 2001). A moderate seasonal pattern is observed in the

estimated contributions of this source to PM10 concentrations, with higher concentrations in summer (Figs. 7 and 8). Both the enhanced photochemistry and the higher air circulation in summer, which favour the formation of secondary sulphates and their distribution on the regional area, can explain this behaviour.

The secondary nitrates source is characterised by nitrates as main tracer; major contributors are nitrates, ammonium and OC, which together account for about 70% of the mass in the factor profile (Fig. 6). This factor shows a strong seasonality, with higher values during the cold period, from November to March, and very low contributions in summertime (Figs. 7 and 8). This behaviour may be due not only to higher emissions, but also to lower mixing layer heights, which favour accumulation of local pollutants near the surface, and lower temperatures, which foster the particulate phase of nitrates and reduce the impact of negative sampling artefacts, whereas nitrate volatilisation is known to be produced by higher temperatures (Chow et al., 2005).

The sea-salt source profile is traced by typical marine elements like Na, Cl and, to a lesser extent, Mg and Br (Fig. 6), with inter-elemental ratios (Na/Cl: 0.56, Mg/Na: 0.13, S/Na: 0.09) in agreement with those reported in literature for seawater (Bowen, 1979). The time pattern is characterised by short episodic peaks (Fig. 7), occurring when air masses are directly transported by strong winds to CA_UB site from the seaside (mainly from the Tyrrhenian Sea). PMF also identified an aged sea salt source, characterised by sea salt elements like Na, Mg and Br, but completely depleted in Cl and enriched in sulphates, nitrates and OC (Fig. 6). It is well known that different heterogeneous reaction between airborne sea-salt particles and gaseous pollutants, like nitric and sulphuric acid, may lead to Cl volatilization and nitrates and sulphates formation (Seinfeld, 1986; Singh, 1995).

As it can be observed in Fig. 8 and Table S2, in Capannori biomass burning is the source that provides the main contribution to PM10; on average, it accounts for the 37% of the PM10 mass (corresponding to 13.7 μg/m^3) and, most important, its contribution increases during the most polluted periods: 52% in winter and 56% during exceedances days, when the average PM10 mass concentration is 65 μg/m^3 and 74 μg/m^3, respectively. Due to the importance of this source, a robust identification of its origin, as well as an accurate quantification of its contribution, are particularly important for this sampling site. To test the stability of the selected PMF solution and quantify the source apportionment uncertainties, the bootstrapping method was used (100 runs, 0.5 min. correlation R-value). Source contributions of the selected solution were within the bootstrap interquartile range for all the sources; the relative uncertainties of the average source contributions (estimated as bootstrap interquartile ranges) were: 5% for BB, 12% for traffic, 5% for soil, 11% for secondary sulphates, 8% for secondary nitrates, 7% for sea salt and 9% for aged sea salt. In particular, the following values were obtained from the bootstrap statistics for the average BB contribution: median 13.6 μg/m^3 (corresponding to 37% of PM10 mass concentration), 5th percentile 11.9 μg/m^3 (32%), 25th perc. 13.2 μg/m^3 (35%), 75th perc. 13.9 μg/m^3 (37%), 95th perc. 16.5 μg/m^3 (44%).

With a 6-factors solution, the two sea salt sources are merged, but the profile and contribution of the other sources do not change significantly; in particular the BB weight (32%) is a bit lower but substantially in agreement, within estimated uncertainties, with that obtained in the 7-factors solution. Very similar results are obtained also in the case when PMF is run with K$^+$ ion instead of K: the same 7 factors are obtained with very similar source profiles and contributions. In particular, the BB average contribution to PM10 is just slightly lower (35% instead of 37%), but completely in agreement within the estimated uncertainties.

PMF analysis of hourly data confirmed and reinforced the above discussed source identification. The analysis was applied separately to the fine and to the coarse aerosol modes and also to the sum of the two fractions. Concerning the latter case, a 5-factors solution has been selected. Most of the scaled residuals are between ± 2.0, with a random

distribution of positive and negative values, and concentrations of all species are reconstructed by the model within 10%. On the basis of their profiles and time series, factors have been assigned to the following aerosol sources: biomass burning (mainly traced by K), traffic (Fe, Cu), soil dust (Al, Si, Ca), secondary sulphates (S) and sea salt (Na, Mg and Cl). The absence of the secondary nitrates source is due to the fact that streaker samples can not be analysed by IC to obtain nitrates concentration (the sulphates source is on the contrary identified as traced by elemental S). One marine aerosol source is identified by this analysis, with elemental ratios typical of fresh sea salt (Na/Cl ~0.6); as can be seen in Fig. 5, no significant Cl depletion is indeed observed during this week, and this explains the absence of an aged sea salt source (it is useful recalling here that hourly samples have been collected only for 1 week in wintertime). In the PMF analysis of the fine fraction, 4 of these sources have been identified: biomass burning, traffic, soil dust and secondary sulphate. For the coarse fraction the biomass burning and secondary sulphate sources have not been detected, as they mainly produce aerosol particles smaller then 2.5 μm, while the sea salt source comes out.

In particular, PMF applied to hourly data confirms the identification of the BB source. This source is found both in the fine fraction and in the sum of the two fractions. Elements more correlated to this source are (the correlation coefficient is reported in brackets): K (0.98), Cl (0.95), Zn (0.83), Ni (0.83), Cu (0.73), Br (0.70) and Pb (0.67) in the fine mode; K (0.97), Ni (0.85), Zn (0.79), Br (0.75), Pb (0.71), S (0.66) and Cu (0.62) in the sum of the two fractions. The time series of the BB source contributions in the fine and in the sum mode are reported in Fig. 9, together with K concentration values in the fine fraction. They are strongly correlated among each other (correlation coefficient 0.97) and with fine K, as just mentioned. Comments on this time pattern are therefore the same as those reported in Section 3.2 about potassium hourly time trend. The periodic behaviour with peaks starting at about 18:00 and the higher values registered during the weekend further support the identification of this source as a BB for domestic heating.

4. Conclusions

The application of PMF on both daily and hourly aerosol composition data sets allowed a clear identification and assessment of an unexpected high biomass burning contribution in an urban background site in Tuscany (central Italy), which also resulted the most polluted among the six sampling sites of the PATOS project. Biomass burning turned out to be the main source of particulate matter, accounting for 37% of the PM10 mass as annual average. During winter, which is the most polluted period (with an average PM10 concentration of 65 μg/m^3), this source contributes to more than 50% of PM10 mass and it is the main cause of all the PM10 limit exceedances. To our current knowledge, while the relevance of biomass burning emissions on PM in many urban and suburban environments in central and northern Europe, also including Northern Italy, has been demonstrated by several studies, it is the first time that a strong impact of this source is found and quantified in central Italy.

In particular, the present work takes advantage of the synergic use of long-term daily data and high time resolution and size-segregated data collected for a shorter period. Daily samples, which have been collected for one year and analysed by different techniques to determine elements, ions and carbon fractions, allowed a reliable source apportionment by PMF and provided insights on the seasonal time trend of the identified sources. In particular, the biomass burning source resulted to be clearly characterised by a very strong seasonality with higher values during the cold season, supporting its interpretation as a combustion source for domestic heating. Hourly samples, collected for a shorter period during wintertime and analysed by PIXE, confirmed and reinforced the identification of this source. In fact, the hourly time pattern of this source (and of all the elemental tracers of biomass burning) was characterised by a periodic behaviour with peaks starting
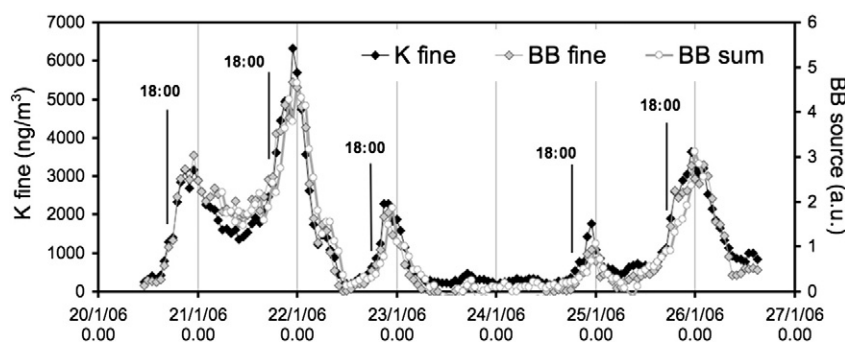
Fig. 9. Hourly time series of the BB source contributions assessed by PMF analysis on the fine fraction ("BB fine") and on the sum of the fine and coarse fractions ("BB sum"); K concentration values are also reported for comparison.

at about 18:00 and lasting for all the evening-night, with higher values during the weekend. Previous studies in Southern European countries identified wildfires and agricultural wastes burning as being likely important biomass combustion sources (Oliveira et al., 2007; Pio et al., 2008; Alves et al., 2011): in this study, the seasonal and hourly time patterns of the identified biomass burning source suggest the absence of important contributions from these processes.

For future studies, the adopted approach could be further reinforced by the simultaneous assessment of specific organic components, like levoglucosan, which, despite its volatility, has been proved to be an effective unique tracer of BB, and radiocarbon analysis (Bernardoni et al., 2013).

Acknowledgements

Appendix A. Supplementary data

Supplementary data to this article can be found online at http://dx.doi.org/10.1016/j.scitotenv.2014.11.034.

References

Akagi SK, Yokelson RJ, Wiedinmyer C, Alvarado MJ, Reid JS, Karl T, et al. Emission factors for open and domestic biomass burning for use in atmospheric models. Atmos Chem Phys 2011;11:4039–72. http://dx.doi.org/10.5194/acp-11-4039-2011.

Alves C, Vicente A, Nunes T, Gonçalves C, Fernández AP, Mirante F. Summer 2009 wildfires in Portugal: Emission of trace gases and aerosol composition. Atmos Environ 2011;40:162–7.

Amato F, Nava S, Lucarelli F, Querol X, Alastuey A, Baldasano JM, et al. A comprehensive assessment of PM emissions from paved roads: real world emission factors and intense street cleaning trials. Sci Total Environ 2010;408:4309–18.

Amato F, Viana M, Richard A, Furger M, Prévôt ASH, Nava S, et al. Size and time-resolved roadside enrichment of atmospheric particulate pollutants. Atmos Chem Phys 2011; 11:2917–31.

Andreae MO, Fishman J, Lindesay J. The southern tropical atlantic region experiment (stare): Transport and atmospheric chemistry near the equator-atlantic (trace a) and southern african fire-atmosphere research initiative (safari): An introduction. J Geophys Res Atmos 1996;101:23519–20.

Becagli S, Ghedini C, Peeters S, Rottiers A, Traversi R, Udisti R, et al. MBAS (Methylene Blue Active Substances) and LAS (Linear Alkylbenzene Sulphonates) in Mediterranean coastal aerosols: sources and transport processes. Atmos Environ 2011;45:6788–801.

Bernardoni V, Vecchi R, Valli G, Piazzalunga A, Fermo P. PM10 source apportionment in Milan (Italy) using time-resolved data. Sci Total Environ 2011;409:4788–95.

Bernardoni V, Calzolai G, Chiari M, Fedi M, Lucarelli F, Nava S, et al. Radiocarbon analysis on organic and elemental carbon in aerosol samples and source apportionment at an urban site in Northern Italy. J Aerosol Sci 2013:88–99.

Bowen HJM. Environmental chemistry of the elements. New York: Elsevier; 1979.

Calastrini F, Guarnieri F, Becagli S, Busillo C, Chiari M, Dayan U, et al. Desert Dust Outbreaks over Mediterranean Basin: A Modeling, Observational, and Synoptic Analysis Approach. Adv Meteorol 2012;2012. http://dx.doi.org/10.1155/2012/246874. [Article ID 246874, 14 pages].

Calzolai G, Chiari M, García-Orellana I, Lucarelli F, Migliori A, Nava S, et al. The new external beam facility for environmental studies at the Tandetron accelerator of LABEC. Nucl Inst Methods Phys Res B 2006;249:928–31.

Chow JC, Watson JG, Lowenthal DH, Magliano KL. Loss of PM2.5 nitrate from filter samples in Central California. J Air Waste Manag Assoc 2005;55:1158–68.

Christensen KA, Stenholm M, Livbjerg H. The formation of submicron aerosol particles, HCl and SO2 in straw-fired boilers. J Aerosol Sci 1998;29:421–44.

Corrigan AL, Russell LM, Takahama S, Äijala M, Ehn M, Junninen H, et al. Biogenic and biomass burning organic aerosol in a boreal forest at Hyytiala, Finland, during HUMPPA-COPEC 2010. Atmos Chem Phys 2013;13:12233–56.

Crespo J, Yubero E, Nicolas J, Lucarelli F, Nava S, Chiari M, et al. High-time resolution and size-segregated elemental composition in high-intensity pyrotechnic exposures. J Hazard Mater 2010. http://dx.doi.org/10.1016/j.jhazmat.2012.09.017.

D'Alessandro A, Lucarelli F, Mandò PA, Marcazzan G, Nava S, Prati P, et al. Hourly elemental composition and source identification of fine and coarse PM10 particulate matter in four Italian towns. J Aerosol Sci 2003;34:243–59.

Dall'Osto M, Querol X, Amato F, Karanasiou A, Lucarelli F, Nava S, et al. Hourly elemental concentrations in PM2.5 aerosols sampled simultaneously at urban background and road site. Atmos Chem Phys 2013;13:4375–92.

Favez O, Cachier H, Sciare J, Sarda-Estève R, Martinon L. Evidence for a significant contribution of wood burning aerosols to PM2.5 during the winter season in Paris, France. Atmos Environ 2009;43:3640–4.

Gelencsér A, May B, Simpson D, Sánchez-Ochoa A, Kasper-Giebl A, Puxbaum H. Source apportionment of PM2.5 organic aerosol over Europe: primary/secondary, natural/anthropogenic, fossil/biogenic origin. J Geophys Res 2007;112(D23):D23S04.

Giannoni M, Martellini T, Del Bubba M, Gambaro A, Zangrando R, Chiari M, et al. The use of levoglucosan for tracing biomass burning in PM2.5 samples in Tuscany (Italy). Environ Pollut 2012;167:7–15.

Gonçalves C, Alves C, Pio C. Inventory of fine particulate organic compound emissions from residential wood combustion in Portugal. Atmos Environ 2012;50:297–306.

Grosjean D. Formic and acetic acids: emissions, atmospheric formation and dry deposition at two southern California locations. Atmos Environ 1992;26A:3279–86.

Jöller M, Brunner T, Obernberger I. Modeling of aerosol formation during biomass combustion for various furnace and boiler types. Fuel Process Technol 2007;88: 1136–47.

Karanasiou AA, Siskos PA, Eleftheriadis K. Assessment of source apportionment by Positive Matrix Factorization analysis on fine and coarse urban aerosol size fractions. Atmos Environ 2009;43:3385–95.

Khalil MAK, Rasmussen RA. Tracers of wood smoke. Atmos Environ 2003;37:1211–22.

Lucarelli F, Nava S, Calzolai G, Chiari M, Udisti R, Marino F. Is PIXE still a useful technique for the analysis of atmospheric aerosols? The LABEC experience. X-Ray Spectrom 2010;40:162–7.

Lucarelli F, Calzolai G, Chiari M, Giannoni M, Mochi D, Nava S, et al. The upgraded external-beam PIXE/PIGE set-up at LABEC for very fast measurements on aerosol samples. Nucl Inst Methods Phys Res B 2014;318:55–9.

Maenhaut W, Raes N, Wang W. Analysis of atmospheric aerosols by particle-induced X-ray emission, instrumental neutron activation analysis, and ion chromatography. Nucl Inst Methods Phys Res B 2011;269:2693–8.

Mason B. Principles of Geochemistry. 3rd ed. New York: Wiley; 1966.

Minguillón MC, Perron N, Querol X, Szidat S, Fahrni SM, Alastuey A, et al. Fossil versus modern sources of fine elemental and organic carbonaceous particulate matter during DAURE campaign in Northeast Spain. Atmos Chem Phys 2011;11: 12067–84.

Nava S, Becagli S, Calzolai G, Chiari M, Lucarelli F, Prati P, et al. Saharan dust impact in central Italy: An overview on three years elemental data records. Atmos Environ 2012;60:444–52.

Obernberger I. Decentralized biomass combustion: state of the art and future development. Biomass Bioenergy 1998;14:33–56.

Oliveira C, Pio C, Alves C, Evtyungina M, Santos P, Gonçalves V. Seasonal distribution of polar organic compounds in the urban atmosphere of two large cities from the North and South of Europe. Atmos Environ 2007;41:5555–70.

Paatero P, Tapper U. Positive matrix factorization: a non-negative factor model with optimal utilization of error estimates of data values. Environmetrics 1994;5:111–26.

Pacyna JM, Pacyna EG. An assessment of global and regional emissions of trace metals to the atmosphere from anthropogenic sources worldwide. Environ Rev 2001;9: 269–98.

Pastorello C, Caserini S, Galante S, Dilara P, Galletti F. Importance of activity data for improving the residential wood combustion emission inventory at regional level. Atmos Environ 2011;45:2869–76.

Piazzalunga A, Belis C, Bernardoni V, Cazzuli O, Fermo P, Valli G, et al. Estimates of wood burning contribution to PM by the macro-tracer method using tailored emission factors. Atmos Environ 2011;45:6642–9.

Pio CA, Legrand M, Alves CA, Oliveira T, Afonso J, Caseiro A. Chemical composition of atmospheric aerosols during the 2003 summer intense forest fire period. Atmos Environ 2008;42:7530–43.

Polissar AV, Hopke PK, Paatero P. Atmospheric aerosol over Alaska: 2. Elemental composition and sources. J Geophys Res 1998:19045–57.

Puxbaum H, Caseiro A, Sánchez-Ochoa A, Kasper-Giebl A, Claeys M, Glencsér A, et al. Levoglucosan levels at background sites in Europe for assessing the impact of biomass combustion on the European aerosols background. J Geophys Res 2007;112:D23S05.

Rahn KA. Silicon and aluminum in atmospheric aerosols: crust-air fractionation? Atmos Environ 1976;10:597–601.

Reche C, Viana M, Amato F, Alastuey A, Moreno T, Hillamos R, et al. Biomass burning contributions to urban aerosols in a coastal Mediterranean city. Sci Total Environ 2012;427–428:175–90.

Reimann C, Ottesen RT, Andersson M, Arnoldussen A, Koller F, Englmaier P. Element levels in birch and spruce wood ashes — green energy? Sci Total Environ 2008;393:191–7.

Rogge WF, Mazurek MA, Hildemann LM, Cass GR. Quantification of urban organic aerosols at a molecular level: identification, abundance and seasonal variation. Atmos Environ 1993;27:1309–30.

Saarikoski SK, Sillanpää MK, Saarnio KM, Hillamo RE, Pennanen AS, Salonen RO. Impact of biomass Combustion on urban fine particulate matter in central and northern Europe. Water Air Soil Pollut 2008. http://dx.doi.org/10.1007/s11270-008-9623-1.

Seinfeld JH. Atmospheric chemistry and physics of air pollution. New York: Wiley; 1986.

Sillapapiromsuk S, Chantara S, Tengjaroenkul U, Prasitwattanaseree S, Prapamontol T. Determination of PM10 and its ion composition emitted from biomass burning in the chamber for estimation of open burning emissions. Chemosphere 2013;93: 1912–9.

Singh HB. Composition, chemistry and climate of the atmosphere. New York: Van Nostrand Reinhold; 1995.

Szidat S, Jenk TM, Synal H-A, Kalberer M, Wacker L, Hajdas I, et al. Contributions of fossil fuel, biomass-burning, and biogenic emissions to carbonaceous aerosols in Zurich as traced by 14C. J Geophys Res 2006;111:D07206. http://dx.doi.org/10.1029/2005JD006590.

Szidat S, Prévôt ASH, Sandradewi J, Alfarra MR, Synal HA, Wacker L. Dominant impact of residential wood burning on particulate matter in Alpine valleys during winter. Geophys Res Lett 2007;34:L05820. http://dx.doi.org/10.1029/2006GL028325.

Szidat S, Ruff M, Perron N, Wacker L, Synal H-A, Hallquist M, et al. Fossil and non-fossil sources of organic carbon (OC) and elemental carbon (EC) in Göteborg, Sweden. Atmos Chem Phys 2009;9:1521–35.

Traversi R, Becagli S, Calzolai G, Chiari M, Giannoni M, Lucarelli F, et al. A comparison between PIXE and ICP-AES measurements of metals in aerosol particulate collected in urban and marine sites in Italy. Nucl Inst Methods Phys Res B 2014;318:130–4.

Viana M, Kuhlbusch TA, Querol X, Alastuey A, Harrison RM, Hopke PK, et al. Source apportionment of PM in Europe: a review of methods and results. J Aerosol Sci 2008;2008:827–49.

Viana M, Reche C, Amato F, Alastuey A, Querol X, Moreno T, et al. Evidence of biomass burning aerosols in the Barcelona urban environment during winter time. Atmos Environ 2013;72:81–8.

Wang Y, Zhuang G, Chen S, An Z, Zheng A. Characteristics and sources of formic, acetic and oxalic acids in PM2.5 and PM10 aerosols in Beijing, China. Atmos Res 2007;84: 169–81.

Zappoli S, Andracchio A, Fuzzi S, Facchini MC, Gelencsér A, Kiss G, et al. Inorganic, organic and macromolecular components of fine aerosol in different areas of Europe in relation to their water solubility. Atmos Environ 1999;33:2733–43.